DTU Library

Ship Roll Motion Control

Perez, Tristan; Blanke, Mogens

[Link back to DTU Orbit](#)

Ship Roll Motion Control

Tristan Perez [*,***] Mogens Blanke [**,***]

* School of Engineering, Discipline of Mechanics and Mechatronics,
The University of Newcastle, Callaghan NSW 2308, AUSTRALIA.

** Department of Electrical Engineering, Automation and Control
Group, Technical University of Denmark (DTU), DK-2800 Kgs.
Lyngby, Denmark.

*** Centre for Ships and Ocean Structures (CeSOS), Norwegian
University of Science and Technology (NTNU), Trondheim, NO-7491,
NORWAY

Abstract: The technical feasibility of roll motion control devices has been amply demonstrated for over 100 years. Performance, however, can still fall short of expectations because of deficiencies in control system designs, which have proven to be far from trivial due to fundamental performance limitations. This tutorial paper presents an account of the development of various ship roll motion control systems and the challenges associated with their design. The paper discusses how to assess performance, the applicability of different models, and control methods that have been applied in the past.

1. INTRODUCTION

Roll motion affects the performance of seagoing surface vessels by limiting the effectiveness of the crew and also the operation of on-board equipment. From William Froude's observations on roll motion, which lead to the proposal of bilge keels in the late 1800s, to the present, various devices have been proposed and used to reduce ship roll motion. Most of these stabilisation devices rely on feedback control systems whose designs have proven to be far from trivial and subject to fundamental performance limitations and trade-offs.

The technical feasibility of roll motion control devices has been amply demonstrated for over 100 years. After the last addition of rudder roll damping systems in the 1970s and 1980s, most of the work shifted to developments in control system design rather than to the development of new stabilisation concepts. Recently, however, there has been a surge in revitalising roll gyrostabilisers and a proposal for zero-speed fin stabilisers. These developments have been push by the luxury yacht industry. In addition, there are currently several navies pursuing again for the use of rudder-roll damping systems.

Most roll motion control devices rely on feedback control systems. This tutorial paper presents an account of the development of various ship roll motion control systems and the challenges associated with their design.

2. SHIP DYNAMICS AND ROLL MOTION

The dynamics of marine vessels can be described using the following general model structure (Fossen, 1994):

$$\dot{\boldsymbol{\eta}} = \mathbf{J}(\boldsymbol{\eta})\,\boldsymbol{\nu}, \tag{1}$$

$$\mathbf{M}_{RB}\,\dot{\boldsymbol{\nu}} + \mathbf{C}_{RB}(\boldsymbol{\nu})\boldsymbol{\nu} = \boldsymbol{\tau}_h + \boldsymbol{\tau}_c + \boldsymbol{\tau}_d, \tag{2}$$

where the vector variables $\boldsymbol{\eta}$ and $\boldsymbol{\nu}$ represent the generalized displacement and body-fixed velocities, and $\boldsymbol{\tau}_h$, $\boldsymbol{\tau}_c$, and $\boldsymbol{\tau}_d$ represent the hydrodynamic, control and disturbance forces respectively. A reference frame $\{b\}$ is considered fixed to the vessel at the point o_b, and a local geographical frame $\{n\}$ is considered fixed to the mean water level at the location o_n. The generalised position and velocity vectors are given by

$$\boldsymbol{\eta} = [n, e, d, \phi, \theta, \psi], \tag{3}$$

$$\boldsymbol{\nu} = [u, v, w, p, q, r]^T \tag{4}$$

The components of $\boldsymbol{\eta}$ are the north, east and down positions of o_b in $\{n\}$ and the Euler angles ϕ-roll, θ-pitch, and ψ-yaw that take $\{n\}$ into the orientation of $\{b\}$. The components of $\boldsymbol{\nu}$ are the linear body-fixed velocities u-surge, v-sway, and w-heave and the components of angular velocity vector are the p-roll rate, q-pitch rate, and r-yaw rate. The generalised force vectors in body-fixed the frame are given by

$$\boldsymbol{\tau}_i = [X_i, Y_i, Z_i, K_i, M_i, N_i]^T, \tag{5}$$

where X_i is the surge force, Y_i is the sway force, Z_i is the heave force, K_i is the roll moment, M_i is the pitch moment, and N_i is the yaw moment. All the moments are taken about o_b.

The kinematic transformation $\mathbf{J}(\boldsymbol{\eta})$ relates the body-fixed velocities to the time derivative in $\{n\}$ of the generalised positions, which gives the vessel trajectory. The matrix $\mathbf{M}_{RB}$ in (2) is the rigid-body mass matrix, and $\mathbf{C}_{RB}(\boldsymbol{\nu})$ is the Coriollis-centripetal matrix. For further details about

general models of marine vessels see Fossen (1994), Fossen (2002), or Perez (2005).

The study of roll motion dynamics for control system design is normally done in terms of either one and four degrees of freedom (DOF) models. The choice between models of different complexity depends on the type of motion control system considered and the conditions under which the design is to be performed. There may be cases where a full six degree of freedom model is required.

2.1 One-degree-of-freedom Model

For a 1DOF model in roll, the model (1)-(2) takes the following form

$$\dot{\phi} = p, \tag{6}$$

$$I_{xx}\,\dot{p} = K_h + K_c + K_d, \tag{7}$$

where I_{xx} is moment of inertia about the x-axis of $\{b\}$. The hydrodynamic forces are approximated by the following parametric model:

$$K_h \approx K_{\dot{p}}\,\dot{p} + K_p p + K_{p|p|}\,p|p| + K(\phi). \tag{8}$$

The first term on the right-hand side of (8) represent a hydrodynamic moment in roll due pressure change that is proportional to the roll accelerations, and the coefficient $K_{\dot{p}}$ is called roll added mass. The second term is damping term, which captures forces due to wave making and linear skin friction, and the coefficient K_p is called a linear damping coefficient. The third term is a nonlinear damping term, which captures forces due to viscous effects, like nonlinear skin friction and eddy making due to flow separation. The last term is a restoring term due to gravity and buoyancy, which for some vessels a linear approximation often suffice:

$$K(\phi) \approx K_\phi\,\phi, \qquad K_\phi = \rho\,g\,\nabla\,GMt, \tag{9}$$

where ρ is the water density, g is the acceleration of gravity, ∇ is the vessel displaced volume, and GMt is the transverse metacentric height.

The coefficients in the hydrodynamic model (8) change with the forward speed of the vessel U. This can be represented in the model by adding terms; for example

$$K_h \approx K_{h0} + K_{hU}, \tag{10}$$

where

$$K_{h0} = K_{\dot{p}}\,\dot{p} + K_p p + K_{p|p|}\,p|p| + K(\phi), \tag{11}$$

$$K_{hU} = K_{Up}\,Up + K_{\phi UU}\,\phi U^2. \tag{12}$$

As the forward speed changes, so does the trim of the vessel, which can be related to the steady state pitch angle. The trim affects not only the damping but also the restoring terms. Some vessels have trim flaps which to correct the trim at different cruise speeds so as to reduce the hydrodynamic resistance and thus reduce fuel consumption. The use of flaps can modify the restoring coefficient.

2.2 Four-degree-of-freedom Model

For a 4DOF model (surge, sway, roll, and yaw), motion variables considered are

$$\boldsymbol{\eta} = [\phi\ \psi]^T, \tag{13}$$

$$\boldsymbol{\nu} = [u\ v\ p\ r]^T, \tag{14}$$

$$\boldsymbol{\tau}_i = [X_i\ Y_i\ K_i\ N_i]^T, \tag{15}$$

The kinematic model (1) reduces to

$$\dot{\phi} = p, \qquad \dot{\psi} = r\cos\phi \approx r. \tag{16}$$

The rigid-body mass and Coriollis-centripetal matrices are given by

$$\mathbf{M}_{RB} = \begin{bmatrix} m & 0 & 0 & -my_g \\ 0 & m & -mz_g & mx_g \\ 0 & -mz_g & I_{xx}^b & -I_{xz}^b \\ -my_g & mx_g & -I_{zx}^b & I_{zz}^b \end{bmatrix}, \tag{17}$$

and

$$\mathbf{C}_{RB}(\nu) =$$
$$\begin{bmatrix} 0 & 0 & mz_g r & -m(x_g r + v) \\ 0 & 0 & -my_g p & -m(y_g r - u) \\ -mz_g r & my_g p & 0 & I_{yz}^b r + I_{xy}^b p \\ m(x_g r + v) & m(y_g r - u) & -I_{yz}^b r - I_{xy}^b p & 0 \end{bmatrix}, \tag{18}$$

where m is the mass of the vessel, $[x_g, y_g, z_g]^T$ gives position the centre of gravity relative to o_b, and I_{ik}^b are the moments and products of inertia about o_b.

The hydrodynamic forces can be expressed as

$$\boldsymbol{\tau}_h \approx -\mathbf{M}_A\,\dot{\boldsymbol{\nu}} - \mathbf{C}_A(\boldsymbol{\nu})\boldsymbol{\nu} - \mathbf{D}(\boldsymbol{\nu})\boldsymbol{\nu} - \mathbf{g}(\boldsymbol{\eta}). \tag{19}$$

The first two terms on the right-hand side of (19) can be explained by considering the motion of the vessel in an irrotational flow and for ideal fluid (no viscosity). As the vessel moves, it changes momentum of the fluid. By considering the kinetic energy of the fluid as $T = 1/2\,\boldsymbol{\nu}^T\mathbf{M}_A\boldsymbol{\nu}$, the first two terms follow from Kirchhoff's equations— see Lamb (1932) and Fossen (1994). The third term in (19) corresponds to damping forces due to potential (wave making), skin friction, vortex shedding, and circulation (lift and drag). The hydrodynamic effects involved are too complex to model. Hence, different approaches based on superposition of either odd-term Taylor expansions or square modulus $(x|x|)$ series expansions are usually used as proposed by Abkowitz (1964) and Fedyaevsky and Sobolev (1964) respectively. The last term in (19) represents the restoring forces in roll due to buoyancy and gravity, which for the DOF considered reduce to (9).

The added mass matrix and the Coriollis-centripetal matrix due to added mass are given by

$$\mathbf{M}_A = \mathbf{M}_A^T = -\begin{bmatrix} X_{\dot{u}} & 0 & 0 & 0 \\ 0 & Y_{\dot{v}} & Y_{\dot{p}} & Y_{\dot{r}} \\ 0 & K_{\dot{v}} & K_{\dot{p}} & K_{\dot{r}} \\ 0 & N_{\dot{v}} & N_{\dot{p}} & N_{\dot{r}} \end{bmatrix}, \tag{20}$$

$$\mathbf{C}_A(\boldsymbol{\nu}) = \begin{bmatrix} 0 & 0 & 0 & Y_{\dot{v}}v + Y_{\dot{p}}p + Y_{\dot{r}}r \\ 0 & 0 & 0 & -X_{\dot{u}}u \\ 0 & 0 & 0 & 0 \\ -Y_{\dot{v}}v - Y_{\dot{p}}p - Y_{\dot{r}}r & X_{\dot{u}}u & 0 & 0 \end{bmatrix}. \tag{21}$$

The adopted damping terms take into account lift, drag, and viscous effects.

$$\mathbf{D}(\boldsymbol{\nu}) = \mathbf{D}_{LD}(\boldsymbol{\nu}) + \mathbf{D}_V(\boldsymbol{\nu}),$$

where

$$\mathbf{D}_{LD}(\boldsymbol{\nu}) = \begin{bmatrix} 0 & 0 & 0 & X_{rv}\,v \\ 0 & Y_{uv}\,u & 0 & Y_{ur}\,u \\ 0 & K_{uv}\,u & 0 & K_{ur}\,u \\ 0 & N_{uv}\,u & 0 & N_{ur}\,u \end{bmatrix}. \tag{22}$$

$$\mathbf{D}_V(\boldsymbol{\nu}) =$$

$$\begin{bmatrix} X_{u|u|} & 0 & 0 & 0 \\ 0 & Y_{|v|v}\,|v| + Y_{|r|v}\,|v| & 0 & Y_{|v|v}\,|v| + Y_{|r|r}\,|r| \\ 0 & 0 & K_{p|p|} + K_p & 0 & 0 \\ 0 & N_{|v|v}\,|v| + N_{|r|v}\,|v| & 0 & N_{|v|v}\,|v| + N_{|r|r}\,|r| \end{bmatrix}.$$

$$(23)$$

The lift-drag representation (22) is consistent with taking only the 1st order terms derived by Ross (2008), whereas the viscous damping representation (23) follows from Blanke (1981), which is a simplification of the model proposed by Norrbin (1970). Some other models appearing in the literature can have additional terms. In the above damping model we have included all the terms with physical meaning. When these models are derived from data of captive scale-model tests, the coefficients are obtained from regression analysis, and further terms may be incorporated to best fit the experimental data (Blanke and Knudsen, 2006; Perez and Revestido-Herrero, 2010).

The above model in 4DOF is called a *manoeuvring model*, since it can be used to describe vessel manoeuvring characteristics. The hydrodynamic forces are modelled on the assumption that there is no waves. The motion in waves is studied under the assumption that the vessel is not manoeuvring and thus the waves induce a perturbation motion about a steady state sailing condition given by a constant speed and heading. This leads to a so-called *seakeeping model*. The problem of manoeuvring in waves is still the subject of ongoing research. For control design, it is common to consider a combination of manoeuvring and seakeeping models–see Skejic (2008).

2.3 Ocean Waves

Ocean waves are random. Regarding the underlying stochastic model, it is usually assumed that the observed sea surface elevation relative to the mean level, $\zeta(t)$, at a certain location and for short periods of time, is a realisation of a stationary and homogeneous zero mean Gaussian stochastic process. The time periods for which ocean waves can be considered stationary can vary between 20 minutes to 3 hours. For deep water, wave elevation tends to present a Gaussian distribution, as the water becomes shallow nonlinear effects dominate, and the waves become non Gaussian (Ochi, 1998).

Under the stationary and Gaussian assumptions, the sea surface elevation is completely characterised by its Power Spectral Density (PSD) $\Phi_{\zeta\zeta}(\omega)$, commonly referred to as the *wave spectrum*. This contains all the information regarding the sea state since the mean of wave elevation is zero, and the variance is given by area under the spectrum over the range of frequencies $(0, \infty)$.

When a marine craft is at rest, the frequency at which the waves excite the craft coincides with the wave frequency; and thus, the previous description is valid. However, when the craft moves with a constant forward speed U, the frequency observed from the craft differs from the wave frequency. The frequency experienced by the craft is called the *encounter frequency*. The encounter frequency depends not only on the speed of the craft, but also on angle the waves approach:

$$\omega_e = \omega - \frac{\omega^2 U}{g}\cos(\chi). \qquad (24)$$

where, the encounter angle χ defines the sailing condition, namely, Following seas ($\chi = 0$deg), Quartering seas ($0 < \chi < 90$ deg), Beam seas ($\chi = 90$ deg), Bow seas ($90 < \chi < 180$ deg), and Head seas ($\chi = 180$ deg).

The encounter frequency captures a Doppler effect, and this is important since the ship motion response due to wave excitation depends on the frequency. As shown by Price and Bishop (1974), the wave spectrum observed from the sea is

$$\Phi_{\zeta\zeta}(\omega_e) = \frac{\Phi_{\zeta\zeta}(\omega)}{\left|\frac{d\omega}{d\omega_e}\right|} = \frac{\Phi_{\zeta\zeta}(\omega)}{\left|1 - \frac{2\omega U}{g}\cos(\chi)\right|}.$$

2.4 Wave-induced Forces and Motion—Seakeeping Models

The motion of a marine craft in waves is the result of the wave excitation due to the varying distribution of pressure on the hull. Therefore, the wave excitation, as well as the vessel response, will depend not only on the characteristics of the waves—amplitude and frequency—but also on the *sailing conditions*: encounter angle and speed. The wave spectrum, and thus the wave-induced forces can change significantly with the sailing conditions for a give sea state.

Based on linear potential theory, hydrodynamic software is nowadays readily available for the computation of the following frequency response functions:

- $\mathbf{F}(j\omega, \chi, U)$ - Wave elevation to excitation force.
- $\mathbf{G}(j\omega, U)$ - Wave excitation to motion.

These frequency responses, known in the marine jargon as *Response Amplitude Operators* (RAOS) are computed based on linearisation at an equilibrium condition defined by a constant forward speed U and encounter angle χ. Because the motion is in 6DOF,

$$\mathbf{F}(j\omega, \chi) = [F_1(j\omega, \chi, U) \cdots F_6(j\omega, \chi, U)]^T, \quad (25)$$

$$\mathbf{G}(j\omega, U) = \begin{bmatrix} G_{11}(j\omega, U) & \cdots & G_{16}(j\omega) \\ \vdots & & \vdots \\ G_{61}(j\omega, U) & \cdots & G_{66}(j\omega, U) \end{bmatrix}, \quad (26)$$

where the degrees of freedom are identified as 1-surge, 2-sway, 3-heave, 4-roll, 5-pitch, and 6-yaw.

From the above frequency response functions, one can obtain the wave to motion response:

$$\mathbf{H}(j\omega, \chi, U) = \mathbf{G}(j\omega, U)\,\mathbf{F}(j\omega, \chi, U). \qquad (27)$$

such that

$$\delta\boldsymbol{\eta}(j\omega) = \mathbf{H}(j\omega, \chi, U)\zeta(j\omega),$$

where the notation $\delta\boldsymbol{\eta}(j\omega)$ indicates that these are perturbation from the equilibrium state. The response for the degree of freedom i is given by

$$H_i(j\omega, \chi, U) = \sum_{k=1}^{6} G_{ik}(j\omega, U)F_k(j\omega, \chi, U). \qquad (28)$$

Figure 1 shows the roll response of a naval vessel for different encounter angels Perez (2005). As we can see from this figure, changes in wave encounter angle can a significant impact on ship roll motion. This often poses
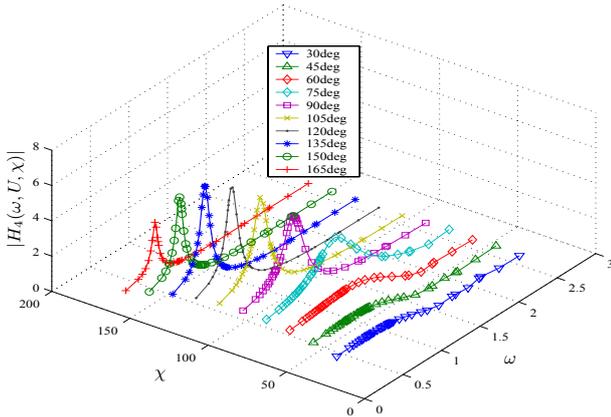
Fig. 1. Roll RAOs of a navy vessel at 15kts for different encounter angles (Perez, 2005).

a problem for roll motion control design since the wave-induced forces and motion are likely to change over a wide range of frequencies depending on sea state and sailing conditions (Blanke et al., 2000).

Potential theory only accounts for damping due to wave making. In the case of roll motion, this can be a small component of the damping since viscous effects may be dominant. This affect the computation of $G_{44}(j\omega, U)$ and thus $H_4(j\omega, \chi, U)$ Hence, one needs to incorporate additional damping. Different empirical methods have been proposed (Ikeda et al., 1976; Ikeda, 2004) (see also Lloyd (1989)). These empirical methods can be used to estimate a linear and quadratic viscous roll damping. An iterative method to obtain an equivalent linearised damping based on energy considerations at a each frequency is described by Lloyd (1989). A counterpart stochastic linearisation method is described in Price and Bishop (1974) and also in Roberts and Spanos (1990). Accurate modeling of damping requires experimental data for parameter estimation.

Having the frequency responses (25)-(26), one can combine them with the wave spectrum to obtain the spectrum of wave-induced forces and wave-induced motion:

$$\Phi_{\tau\tau,i}(j\omega_e) = |F_i(j\omega_e, \chi, U)|^2 \Phi_{\zeta\zeta}(j\omega_e), \qquad (29)$$

$$\Phi_{\eta\eta,i}(j\omega_e) = |H_i(j\omega_e, \chi, U)|^2 \Phi_{\zeta\zeta}(j\omega_e). \qquad (30)$$

These spectra can used to simulate time series of either wave-excitation forces or wave-induced motion. Since the wave elevation is Gaussian and considered stationary, and the force response being considered is linear, then the response is also Gaussian and stationary. One approach to generate realisations from the spectrum consists of making a spectral factorisation of (29) or (30) and approximate the realisations as filtered white noise. This approach is commonly used in stochastic control theory. An approach commonly used in marine engineering is to use a multi-sine signal. For example for any component of η_i, we can generate realisations via

$$\eta_i(t) = \sum_{n=1}^{N} \bar{\eta}_n \cos(\omega_{e,n} t + \varepsilon_n), \qquad (31)$$

with N being sufficiently large, where $\bar{\eta}_n$ are constants, and the phases ε_n are independent identically distributed random variables with uniform distribution in $[0, 2\pi]$. This choice of random phases ensures that $\eta_i(t)$ is a Gaussian process, and for each realisation of the phases, we obtain a realisation of the process (St Denis and Pierson, 1953). The amplitudes are determined from $\bar{\eta}_n = \sqrt{2\Phi_{\eta\eta,i}(\omega^*)\Delta\omega}$, where ω^* is chosen randomly within the interval $[\omega_n - \frac{\Delta\omega}{2}, \omega_n + \frac{\Delta\omega}{2}]$.

In the above account, we have assumed the the sea approaches the vessel from a unique direction given by the encounter angle χ. This is an assumption is in general sufficient to test the performance of ship motion control systems. If a more realistic scenario is desired, one can use a directional wave spectrum $S_{\zeta\zeta}(\omega, \chi)$, and superimpose the response for the different directions. For further details see Perez (2005).

3. ROLL MOTION AND SHIP PERFORMANCE

Roll affects ship performance in terms of preventing the operation of on-board equipment, human performance, and in some case it affects the efficiency of the propulsion system. As discussed in Perez (2005), transverse accelerations due to roll induce interruptions in the tasks performed by the crew. This increases the amount of time required to complete the missions, and in some cases may even prevent the crew from performing tasks at all. This can render navy ships inoperable (Monk, 1988). Vertical accelerations induced by roll at locations away from the ship's centre line can contribute to the development of seasickness in the crew and passengers, which affects performance by reducing comfort. Roll accelerations may produce cargo damage, for example on soft loads such as fruit. Large roll angles limit the capability to handle equipment on board. This is important for naval vessels performing weapon operations, launching or recovering systems, landing airborne systems, and sonar operation.

Within the naval environment, several performance indices and associates criteria are used to quantify ship performance relative to the missions it performs. Among the different performance indices, the following are affected by roll motion (NATO, 2000):

- maximum roll angle, propeller emergence,
- vertical acceleration, lateral force estimator,
- motion sickness incidence and induced interruptions.

From these it follows that the performance of a roll motion control system must be judged not only in terms of roll angle reduction, but also roll accelerations.

4. ROLL DAMPING DEVICES

The undesirable effects of roll motion became noticeable in the mid-19th century when significant changes were introduced to the design and development of ships. Sails were replaced by steam engines, and for warships, the arrangement was changed from broadside batteries to turrets (Goodrich, 1969). The combination of these changes, in particular the dropping of sails, led to modifications of the transverse stability with the consequence of large roll motion.

The increase in roll motion and its effect of ship and human performance lead to a wealth of different devices that aim at reducing and controlling roll motion. The devices most

commonly used today are water tanks, gyro-actuators, fins, and rudder.

In 1878, a committee in England presented a study on damaged stability for the *HMS Inflexible*, in which they concluded that the free flow of the water within the damaged compartments contributed to an increase of roll righting power. This happened only if the number of partially flooded compartments was low and the level of water appropriate (Chalmers, 1931; Goodrich, 1969). As a result of these experiments, the *HMS Inflexible* was permanently fitted with water chambers in 1880 (Watt, 1883, 1885). This, together with the work of Froude, was probably the earliest attempt of using passive anti-rolling tanks. The work described above was followed by the development of the U-tank made by Frahm (1911). This U-tank was found to be more effective than the free-surface tank previously used by Froude and Watt. A U-tank consists of two reservoirs located one on the starboard side an the other on the port side. These reservoirs are connected via duct that allows the flow from one reservoir to the other. This type of anti-roll tank is still very much in use to date. The tanks are dimensioned so that the tank natural frequency matches the vessel roll natural frequency. This can only be achieved at a single frequency. Therefore, performance degradation occurs if the motion of the vessel departs from the natural frequency. This can be circumvented by active control. Work on active anti-roll tanks started in the 1930s. For example, Minorsky (1935) used a pump to alter the natural flow in the tanks in 1934. The velocity of the fluid was varied according to the roll acceleration. During the 1960s and 1970s there was significant research activity to better understand the performance of these stabilisers, see for example, Vasta et al. (1961); Goodrich (1969) and references therein. More complete passages on the history and the development of anti-roll tanks, which also includes contemporary references, can be found in Chalmers (1931); Vasta et al. (1961); Goodrich (1969); Gawad et al. (2001). In particular, the work of Vasta et al. (1961), summarises the early development of stabilisers within the US Navy, which did not take place until the 1930s. This reports the use of tanks in different vessels, and provides a mathematical model of a U-tank based on the developments made at Stanford University in the early 1950s. To date, the control is performed by controlling the air pressure on the upper side of the reservoirs via a valve.

The use of gyroscopic effects was then proposed as a method to eliminate roll rather than reducing it. A gyrostabiliser consists of one or more dedicated spinning wheels whose gyroscopic effects are used to counteract roll excitation forces. Schlick (1904) was the first to propose use of the gyroscopic effects of large rotating wheels as a roll control device. In 1907, this system was installed on the ex-German torpedo-boat destroyer *See-Bar*. The Schlick gyroscope presented some problems in adjusting its performance according to the magnitude of the the waves, and although it worked well for the vessel used by Schlick, it did not perform as expected in other vessels—see Chalmers (1931) for details. The American company Sperry then developed a system that addressed the problem of the Schlick gyroscope by using an electrical motor commanded by switches and a small gyroscope to control the precession

of the main gyroscope. In this, the velocity of precession was proportional to the roll rate of the vessel. Although the performance of these system was remarkable, up to 95% roll reduction, their high cost, the increase in weight and large stress produced on the hull masked their benefits and prevented further developments. In recent years, there has been a increase the development of gyrostabilisers driven by the yacht industry and the need to stabilise roll motion at anchor (Perez and Steinmann, 2009).

Fin stabilisers consist of a pair of controlled hydrofoils mounted on the side of the hull, which are commanded by a control system to produce a roll moment that counteracts the wave induced moment—see Figure 2. The first proposal for fin stabilisers was made by S. Motora of the Mitsubishi Nagasaki Shipyard in Japan, in 1923 (Chalmers, 1931). The use of active-fin stabilisers increased after World War II. This was a consequence of the combined work of the Denny and the Brown Brothers companies in England, but the idea of using fin stabilisers was developed before the war. To date fin stabilisers are also used at zero forward speed–flapping fins.

The idea of using the rudder as a stabilisation device emerged from observations of ship roll behaviour under autopilot operation. Taggart (1970) reported an unusual combination of circumstances occurring on the *American Resolute* (container ship) during a winter Atlantic crossing in 1967, which resulted in excessive ship rolling when automatic steering was used. From data observed during that trip and a model constructed from data of a summer crossing in 1968, it was concluded that the high roll motion observed, even in the absence of significant seaway, was the consequence of high yaw frequencies, which made the autopilot produce rudder activity close to the roll natural frequency of the ship. It was then suggested that the autopilot control system should be modified to avoid these effects; however, the fact that rudder motion could produce large roll could be used as anti-rolling device. Motivated by the observations made by Taggart, van Gunsteren performed full-scale trials using the rudder as a stabiliser in 1972 aboard the motor yacht *M.S. Peggy* in Ijsselmeer (inner waters of The Netherlands). This work was reported by van Gunsteren (1974). Independently from the above work, Cowley and Lambert (1972) presented a study of rudder roll stabilisation using analog computer simulations and model testing of a container ship in 1972. Subsequent sea trials following this work were reported in Cowley (1972); Cowley and Lambert (1975), the latter with encouraging results. This work, obtained on commercial ships, motivated the exploration of rudder stabilisers in the naval environment in the United Kingdom. Carley (1975) and Lloyd (1975a) reported their studies, in which they analysed not only the benefits but also the complications associated with the control of rudder stabilisers. This work seems to have been the first rigorous attempt to analyse performance limitations of rudder stabilisers. Although the idea of using the rudder as a roll stabilising mechanism ignited in the early 1970s, the performance obtained was, in general, poor. This was mainly because of the simple control strategies attempted, due to the limitations imposed by the analog computers. It was only in the 1980s that more advanced control algorithms, and digital computers made more successful experimental results possible: Baitis

reported roll angle reductions of 50% in 1980—see Baitis (1980). After this, most of the successful implementations were reported towards the end of the 1980s and beginning of the 1990s—see for example the work of van der Klught, van der Klught (1987), Källström (1981), Källström et al. (1988) Blanke et al. (1989) and van Amerongen et al. (1990). These developments were mostly within the naval environment.

The above is a brief review on the main developments of stabilisation concepts. Sellars and Martin (1992) provide a comparison between different devices in terms of performance and cost. A more complete account on the historical control aspects can be found in Perez (2005).

5. CONTROL DESIGN AND PERFORMANCE LIMITATIONS

Let us consider the problem of active control of roll motion by means of force actuators within a linear framework and for the decoupled roll motion. We can then define the output sensitivity transfer function:

$$S(s) \triangleq \frac{\phi_{cl}(s)}{\phi_{ol}(s)}, \qquad (32)$$

where $\phi_{cl}(s)$ and $\phi_{ol}(s)$ are the Laplace transforms of the closed- and open-loop roll angles respectively. The control objective then becomes the reduction of the sensitivity within the range of frequency of interest.

Due to the feedback control system, Bode's integral constraint establishes that, when the system is stable and has relative degree strictly larger than one,

$$\int_0^\infty \log |S(j\omega)| \, d\omega = 0. \qquad (33)$$

This constraint indicates that a reduction of the magnitude of the sensitivity below 1 at some frequencies must result in an increase at other frequencies. By defining the roll reduction as

$$RR(\omega) = 1 - |S(j\omega)| = \frac{|\phi_{ol}(j\omega)| - |\phi_{cl}(j\omega)|}{|\phi_{ol}(j\omega)|}, \qquad (34)$$

the integral constraint becomes

$$\int_0^\infty \log(1 - RR(\omega)) \, d\omega = 0. \qquad (35)$$

Furthermore, we can consider the open- and closed-loop responses from wave-induced moment to roll angle,

$$G_{ol}(s) = \frac{\phi_{ol}(s)}{\tau_w(s)}, \qquad (36)$$

$$G_{cl}(s) = \frac{\phi_{cl}(s)}{\tau_w(s)}. \qquad (37)$$

Using these functions we can express the roll reduction as

$$RR(\omega) = \left(1 - \frac{|G_{cl}(j\omega)|}{|G_{ol}(j\omega)|}\right). \qquad (38)$$

We note that $G_{ol}(s)$ depends only on the vessel characteristics, i.e., hydrodynamic aspects and mass distribution. Hence, the integral constraint (35) imposes restrictions on one's freedom to shape the function $G_{cl}(s)$ to attenuate the motion due to the wave induced forces in different frequency ranges. These results have important consequences on the design of a control system. Indeed, since the frequency of the waves seen from the vessel change

significantly with the sea state, the speed of the vessel, and the heading with respect to the wave propagation direction.

For some roll motion control problems, like rudder roll damping and fin stabilisers, the system presents non-minimum phase dynamics. This effect is related to the location of the force actuator and the coupling between different degrees of freedom—roll, sway and yaw. In these cases, there is an integral constraint similar to (33) but the sensitivity reduction-amplification trade off is concentrated to frequency regions in the neighbourhood of the real right half plane (RHP) zero (non-minimum phase zero) located at $s = q$:

$$\int_{-\infty}^\infty \log |S(j\omega)| \, W(q, \omega) d\omega = 0. \qquad (39)$$

The formal prerequisite here is again that the open-loop transfer function of plant and controller has relative degree strictly larger than one and that the open loop has no poles in the right half plane. Both criteria are met for the fin or rudder to roll transfer functions of a vessel with positive metacentric height. The weighting function $W(q, \omega)$ is referred to as the Poisson Kernel, and the above integral is known as the Poisson integral constraint for stable single-single-output feedback systems (Serón et al., 1997) and references therein.

From the constraints (33) and (39), one can obtain bounds on the maximum of the sensitivity that can be expected outside the attenuation range $\Omega_a = [\omega_{min}, \omega_{max}]$. That is if the control requirement is

$$|S(j\omega)| \le \alpha, \quad \text{for } \omega \in \Omega_a, \qquad (40)$$

then,

$$1 \le \|S(j\omega)\|_\infty \le \gamma(q, \Omega_a, \alpha), \text{ for } \omega \notin \Omega_a. \qquad (41)$$

See Perez (2005) and references therein for further details. The above discussion simply shows general design constraints that apply to roll motion control systems in terms of the dynamics of the vessel and actuator. In addition to these constraints, one needs also to account for limitations due to actuator capacity. We further discuss the topic of fundamental limitations in the following sections.

6. ROLL DAMPING DEVICE CONTROL DESIGN

6.1 Fins

The control design for fin stabilisers is normally performed based on a roll linear single degree freedom model,

$$\dot{\phi} = p, \qquad (42)$$

$$K_{\dot{p}} \dot{p} + K_p p + K_\phi \phi = K_w + K_f, \qquad (43)$$

where K_w is wave induced roll moment and K_f is the roll moment induced by the fins.

The lift and drag forces of the hydrofoils are concentrated at the centre of pressure (CP) and can be modeled as

$$L = \frac{1}{2}\rho V_f^2 A_f \bar{C}_L \alpha_e$$
$$D = \frac{1}{2}\rho V_f^2 A_f \left(C_{D0} + \frac{(\bar{C}_L \alpha_e)^2}{0.9\pi a}\right), \qquad (44)$$

where V_f is the flow velocity upstream from the foil, A_f is the area of the foil, α_e is the effective angle of attack
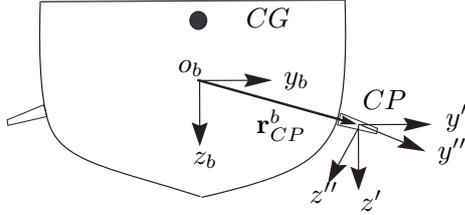
Fig. 2. Reference frames used to compute fin forces.

in radians, and a is the effective aspect ratio. In (44), we have used the linear approximation for the lift coefficient:

$$\bar{C}_L = \left.\frac{\partial C_L}{\partial \alpha_e}\right|_{\alpha_e=0},$$

which is valid for $\alpha_e < \alpha_{stall}$. Once the stall angle of the hydrofoils is reached, the flow separates and the lift reduces.

The lift force is perpendicular to the direction of the relative flow, whereas the drag force is aligned with the relative flow. The computation of the roll moment due to these forces requires taking into account the complete motion of the vessel. To calculate the forces, we consider the reference frames depicted in Figure 2, and we assume that the location of the centre of pressure of the fin in body-fixed coordinates is given by the vector $\mathbf{r}_{CP}^b = [x_{CP}^b, y_{CP}^b, z_{CP}^b]^T$.

If we neglect the influence of pitch and heave motion, then the relative flow in frame x'', y'', z'' is

$$\mathbf{v}_f = [-u, 0, -r_f\, p]^T, \quad r_f = \sqrt{(y_{CP}^b)^2 + (z_{CP}^b)^2}, \quad (45)$$

where u is the forward speed of the vessel, and we are assuming the vessel centre of roll is at the origin of the body-fixed frame. The angle of the flow relative to x'', y'', z'' is defined as

$$\alpha_f = \arctan\frac{r_f p}{u} \approx \frac{r_f p}{u}, \quad (46)$$

and the effective angle of attack is given by

$$\alpha_e = -\alpha_f - \alpha, \quad (47)$$

where α is the mechanical angle of the fin, defined positive defined using the right hand screw rule along the y'' axis: a positive angle means leading edge up: trailing edge down.

The lift and drag forces in x'', y'', z'' are

$$\mathbf{F}_{LD} = [D, 0, L]^T, \quad (48)$$

and the roll moment can then be expresses as

$$X_f = [1, 0, 0]\,\mathbf{S}(\mathbf{r}_{CP}^b)\,\mathbf{R}_{x,\gamma}\,\mathbf{F}_{LD}, \quad (49)$$

where $\mathbf{R}_{x,\gamma}$ is the rotation matrix that takes the b-frame into the orientation of x'', y'', z'' (which we assume that the tilt angle is γ about the x-axis), and $\mathbf{S}(\mathbf{r}_{CP}^b)$ is the skew-symmetric matrix associated with the vector $\mathbf{r}_{CP}^b$. After, calculations, and further approximating $\|\mathbf{v}_f\| \approx u$, we obtain that

$$X_f \approx u^2 K_\alpha\, \alpha_e, \quad (50)$$

where

$$K_\alpha = \frac{1}{2}\rho A_f(y_{CP}^b \cos\gamma - z_{CP}^b \sin\gamma). \quad (51)$$

From the above, we can finally express the model as

$$\dot{\phi} = p, \quad (52)$$

$$K_{\dot{p}}\,\dot{p} + (K_p + 2\,r_f K_\alpha u)\,p + K_\phi\,\phi = K_w - 2u^2 K_\alpha\,\alpha. \quad (53)$$

As we can see from the model, the presence of the fins increase the bare damping of the hull, and the damping as well as the effectiveness of the fins is affected by the forward speed.

From the point of view of control design, the main issues are the parametric uncertainty in (53) and the integral constraints (33), which applies if only roll angle feedback is used. The integral constraint can lead to roll amplification due to changes in the spectrum of the wave-induced roll moment with sea state and sailing conditions. Fin machinery is normally designed so the rate of the fin motion is fast enough so there are no issues of actuator rate saturation. The fins can be used to correct heeling angles (steady state roll). This is achieved by integral action in the controller—which requires anti wind-up implementation to avoid performance degradation due actuator saturation in magnitude.

Classical PID and $\mathcal{H}_\infty$ types of controllers usually perform well (Hickey et al., 1995, 1997, 1999; Hickey, 1999; Katebi et al., 2000), and most of the early literature on fin stabilisation focused strongly on the hydrodynamic aspects of the fins, fin size and location rather than control design (Allan, 1945; Conolly, 1969; Lloyd, 1975b; Dallinga, 1993). These aspects have continued to attract research attention until recent years due to tendency of fins to develop dynamic stall conditions in moderate to severe sea states (Gaillarde, 2002). This latter work has motivated the control strategy proposed in Perez and Goodwin (2008), which considers a constraint on the effective angle of attach to prevent dynamic stall.

Although, the traditional approach for the design of fin stabiliser control consists of using the decoupled roll motion equations, the cross-coupling between roll, sway and yaw often reduces the performance of the fins, and therefore if the system as a whole is to operate optimally, and integrated control for rudder and fin should be considered. What's more, if the fins are located aft, the a non-minimum phase dynamics can appear in the response due to coupling with yaw, which can complicate the controller design and compromise the performance at low encounter frequencies. Non-minimum phase dynamics in fin-roll response and the design trade-offs due to integral constrain (39) were mentioned by Lloyd (1989), and discussed by Perez (2005).

6.2 Rudder Roll Damping

As mentioned in Section 4, using the rudder for simultaneous steering and roll damping has been investigated for several decades. Early results demonstrated the importance of available rudder rate to achieve desired roll damping. Implementation on a number of vessels in different countries showed limitations to achievable roll reduction. A full understanding of the limits due to dynamics of the problem was not available until results on achievable performance for systems appeared Freudenberg and Looze (1985) and further elaborated and extended in Freudenberg and Looze (1988), and Serón et al. (1997).

For roll-damping by the rudder, the linearised transfer function obtained from the 4DOF model specified in Section 2.2 is

$$G_{\phi\delta}(s) = \frac{c_{\phi\delta}(1 + s\tau_{z1})(1 - \frac{s}{q})}{(1 + s\tau_{p1})(1 + s\tau_{p2})(\frac{s^2}{\omega_p^2} + 2\zeta_p\frac{s}{\omega_p} + 1)} \quad (54)$$

With a single, real-valued right-half plane zero, the Poisson kernel in (39) is

$$W(q,\omega) = \frac{q}{q^2 + \omega^2}. \quad (55)$$

If the output disturbance d_ϕ (wave-induced roll motion) is to be attenuated, *i.e.* $\ln|S(j\omega)| < 0$ (or equivalently $|S(j\omega)| < 1$) in a range of frequencies $\omega \in \Omega$, then there must be amplification of disturbances at frequencies outside Ω, *i.e.* for $\omega \notin \Omega$, $\ln|S(j\omega)| > 0$ (or $|S(j\omega)| > 1$). Furthermore, due to the weighting factor in the integral, this balance of area has to be achieved over a limited band of frequencies, which depend on the position of the RHP zero.

Now consider the implications on control system design. Suppose that the feedback loop is to be designed to achieve

$$|S(j\omega)| \le \alpha_1 < 1 , \qquad \forall \omega \in \Omega_1 = [\omega_1, \omega_2]. \quad (56)$$

Define,

$$\Theta_\sigma(\omega_1, \omega_2) \triangleq \int_{\omega_1}^{\omega_2} \frac{q}{q^2 + \omega^2} \, d\omega = \arctan\frac{\omega_2}{q} - \arctan\frac{\omega_1}{q}. \quad (57)$$

Dividing the range of integration in (57), and using the inequality (56) and also the fact that $|S(j\omega)| \le \|S(j\omega)\|_\infty$ for all ω, we obtain that

$$\ln\alpha_1 \, \Theta_\sigma(\omega_1, \omega_2) + \ln\|S(j\omega)\|_\infty [\pi - \Theta_\sigma(\omega_1, \omega_2)] \ge 0. \quad (58)$$

By exponentiating both sides of (58), it follows that

$$\|S(j\omega)\|_\infty \ge \left(\frac{1}{\alpha_1}\right)^{\frac{\Theta_\sigma(\omega_1,\omega_2)}{\pi - \Theta_\sigma(\omega_1,\omega_2)}}. \quad (59)$$

Thus, the right-hand side of (59) is a lower bound on the sensitivity peak that we can expect outside the range $[\omega_1, \omega_2]$. It is immediate from (59) that the lower bound on the sensitivity peak is strictly greater than one: this follows from the fact that $\alpha_1 < 1$ and $\Theta_q(\omega_1, \omega_2) < \pi$. Furthermore, the more the sensitivity is pushed down, i.e., the lower is α_1, and the bigger is the interval $[\omega_1, \omega_2]$, then the bigger $\|S(j\omega)\|_\infty$ will be at frequencies outside that interval.

The above description of the disturbance attenuation problem has been formulated from a deterministic point of view. The use of frequency response is particularly attractive to consider sinusoidal disturbances. Indeed, if the frequency of the disturbance is not known exactly, then the reduction of the sensitivity should be considered over a range of frequencies where the disturbance is likely to be. The price to pay for doing this is an increase of sensitivity outside the range of reduction, and the risk of disturbance amplification if the disturbance is indeed outside the reduction range.

With a fixed controller for rudder roll damping, there is the risk that for some sailing conditions and sea states, the disturbances have significant energy in the frequency ranges where roll is amplified. This is more likely to happen in quartering sailing conditions for which low encounter frequencies result. This would mean having a disturbance with significant energy at frequencies below ω_1.

This limitation had been recognised since the first attempts to use rudder as a roll damping device were made—see Carley (1975); Lloyd (1975a) but the stringent mathematical background was not disclosed until much later, when the analysis of performance limitations due to the RHP zero was approached using the Poisson integral formula, was first presented in Hearns and Blanke (1998a).

Perez (2005) took a state-feedback approach, and formulated the control problem as an optimal control problem, in which the following cost was minimised

$$J = \mathrm{E}[\lambda\phi^2 + (1 - \lambda)(\psi - \psi_d)^2],$$

where $\lambda \in [0, 1]$ represents the desired of reducing roll over yaw deviations. When $\lambda = 1$, it was established that

$$\mathrm{E}[\phi^2] \ge 2\, q\, \Phi_{\phi\phi}(q), \quad (60)$$

where $\Phi_{\phi\phi}(\omega)$ is the open-loop roll spectrum.

Expression (60) shows that the closer the RHP zero is to the imaginary axis, the better are the chances for a rudder stabiliser to perform well. A RHP zero close to the imaginary axis will produce a large initial inverse response to a rudder step command. The fact that a large initial inverse response to a step in the rudder command is an indication of the potential for good performance of a rudder stabiliser has been discussed by Roberts (1993). Therefore, the location of the RHP zero with respect to the imaginary axis gives a *definite* and *quantitative* interpretation for the statement constantly appearing in the literature which says that for a rudder stabiliser to perform well there must be a frequency separation between the roll and yaw responses due to the rudder action. Indeed, if the zero is close to the imaginary axis, this means that there will be a timelag in the development of the hydrodynamic moment acting on the hull that opposes that produced by the rudder. For a given ship, the location of the RHP zero is determined by its hydrodynamic parameters. The relation between hydrodynamic parameters was derived from PMM data for a container vessel by Hearns and Blanke (1998b).

Equation (60) also shows another important aspect: a RHP zero close to the imaginary axis does not *per se* guarantee good performance; there must also be a frequency separation between the RHP zero and the bulk of power of the wave-induced roll motion in order to achieve good performance. This answers the question as to why RRD systems can have significantly different performance under different sailing conditions, with poor performance being particularly noticeable at low-encounter frequencies.

The bound on the right-hand side of (60) is very conservative because there is no penalty in the control energy used. A more realistic bound was also considered in Perez (2005), by imposing a constraint on the variance of the rudder angle, such that the maxima of rudder angle exceed a certain threshold value with low probability. Perez (2005) also presented a curves of potential roll reduction *vs* yaw interference for a sea state and sailing conditions, which could be used to benchmark performance of the final control designs.
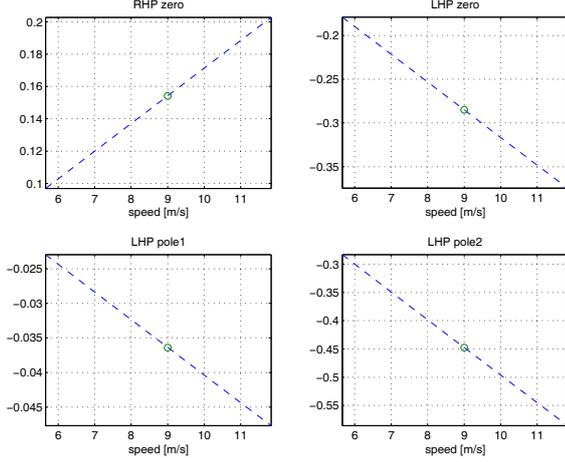
Fig. 3. Change of poles and zeros with ship speed.

With the importance of the location of the RHP zero, it is essential to know the variation of its location as a function of various parameters of the ship. Using model and data from Blanke and Christensen (1993), Figure (3), shows the change of the location of both the RHP zero and the LHP pole/zeroes of (54) when ship speed is changed. The nominal is indicated by an "o" in the Figures. The RHP variation is significant with ship speed and also with vertical location of the meta-centre. The latter will change with the loading condition and trim of the vessel.

While the RHP zero is limiting the maximal achievable damping, actual achievable damping is determined by the magnitude of the sensitivity function $S(j\omega)$ in Eq. (34), which also depends of the remaining dynamics. A controller that achieves the minimal variance in roll in closed loop was derived in Perez (2005). Given a motion spectrum $\Phi_{\phi\phi}(\omega)$ with a spectral factorisation

$$\Phi_{\phi\phi}(\omega) = H_d^*(j\omega)H_d(j\omega), \qquad (61)$$

define a modified rudder to roll transfer function with the right half plane zero mirrored to the left half plane

$$G_{\phi\delta}^-(s) = G_{\phi\delta}(s)\frac{s+q}{s-q}. \qquad (62)$$

Determine also the stable part of the product

$$H_d(s)\frac{s+q}{s-q} = \sum_{p_i<0}\frac{a_i}{1+\frac{s}{p_i}} + \sum_{p_j\geq0}\frac{a_j}{1+\frac{s}{p_j}} \qquad (63)$$

$$= H_d^-(s) + H_d^+(s). \qquad (64)$$

Then the best achievable roll damping is obtained by the controller (Perez (2005))

$$Q(s) = (H_d(s)G_{\phi\delta}^-(s))^{-1}H_d^-(s) \qquad (65)$$

$$C_{\delta\phi}(s) = \frac{Q(s)}{1 - G_{\phi\delta}(s)Q(s)} \qquad (66)$$

$$RR_{opt}(s) = G(s)Q(s) \qquad (67)$$

$$= H_d^-1H_d^-\frac{s-q}{s+q} \qquad (68)$$

Inserting in the expressions for $Q(s)$ into $C_{\delta\phi}(s)$ gives

$$C_{\delta\phi}(s) = (G^-)^{-1}\frac{H_d^{-1}H_d^-}{1 - \frac{s-q}{s+q}H_d^{-1}H_d^-}, \qquad (69)$$

This controller is stable but non-causal. A realizably suboptimal control could be obtained by padding necessary poles on the controller. The controller is rather sensitive to the exact form of the $H_d^{-1}H_d^-$ term and would require accurate estimation of the sea-generated motion, which means an adaptive solution would be needed.

As an illustration, if

$$H_d(s) = \frac{\omega_w^2}{s^2 + 2\zeta_w\omega_w s + \omega_w^2}, \qquad (70)$$

then

$$H_d^-(s) = -\frac{sa+b}{s^2 + 2\zeta_w\omega_w s + \omega_w^2}, \qquad (71)$$

with parameters

$$b = \omega_w^2\frac{-\omega_w^2 + 2q\zeta_w\omega_w + q^2}{\omega_w^2 + 2q\zeta_w\omega_w + q^2} \qquad (72)$$

$$a = \frac{2q\omega_w^2}{\omega_w^2 + 2q\zeta_w\omega_w + q^2}. \qquad (73)$$

Hence, the product $H_d^{-1}H_d^- = as + b\omega_w^{-}2$ and the theoretical result for roll reduction

$$RR = \frac{as+b}{\omega_w^2}\frac{s-q}{s+q}, \qquad (74)$$

which would be optimal for the wave model specified, but not obtainable.

An appealing alternative is to instead calculate the controller directly from a specification of desired sensitivity function $S(\omega)$.

The form of the sensitivity function for roll damping should asymptotically approach one at high and very low frequencies, for reasons of the Poisson integral condition and for reasons of physics. Attempting to reduce roll at high frequencies is impossible, reducing at very low frequencies would prevent the natural heel required during a turn of a ship and would deteriorate manoeuvring capability. Damping should be high in the frequency range of sea-induced motion. Therefore, the desired sensitivity function can be chosen of the form

$$S_d(s) = \frac{\frac{s^2}{\omega_d^2} + 2\zeta_d\frac{s}{\omega_d} + 1}{(1 + \frac{s}{\beta\omega_d})(1 + \frac{\beta s}{\omega_d})}. \qquad (75)$$

With control action (rudder angle) $\delta(s) = C_{\delta\phi}(s)\phi(s)$ the sensitivity to roll motion disturbance is

$$S(s) = (1 + C_{\delta\phi}(s)G_{\phi\delta}(s))^{-1} \qquad (76)$$

The stable controller required to obtain a desired specification as well as possible is

$$C_{\delta\phi}^s(s) = (S_d(s)^{-1} - 1)G_{\phi\delta}^{-1}(s)\frac{1 - \frac{s}{q}}{1 + \frac{s}{q}}P(s)^{-1} \qquad (77)$$

where $P(s)$ is a polynomium comprising any poles needed for realizability of $C_{\delta\phi}^s(s)$. The specification obtainable is

$$S_{obtained}(s)^{-1} = 1 + (S_d(s)^{-1} - 1)\frac{1 - \frac{s}{q}}{1 + \frac{s}{q}}P^{-1}(s) \qquad (78)$$

This best possible controller, given the specification (75) and the linear rudder to roll dynamics (54), takes the form
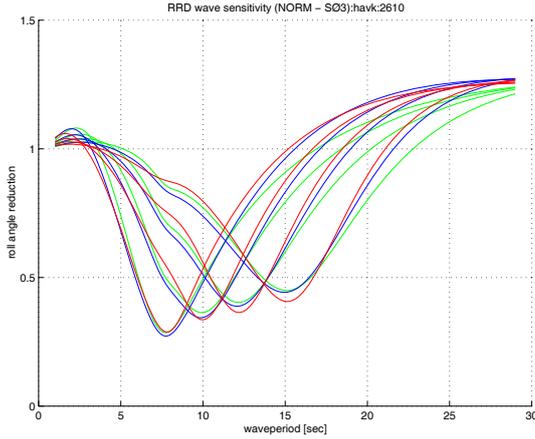
Fig. 4. Specification driven design in practice with four different tunings of the parameter $2\pi/\omega_d$ set to 8, 10, 12 and 15 sec, respectively. Three different settings of the sea-filter of the heading controller are shown, to validate robustness.

$$C_{\delta\phi}^s(s) = \frac{sk_1}{c_{\phi\delta}\omega_d} \frac{\frac{s^2}{\omega_p^2} + 2\zeta_p \frac{s}{\omega_p} + 1}{\frac{s^2}{\omega_d^2} + 2\zeta_d \frac{s}{\omega_d} + 1} \frac{(1 + s\tau_{p1})(1 + s\tau_{p2})}{(1 + s\tau_{z1})(1 + \frac{s}{q})},$$
(79)

where $k_1 = (\beta + \beta^{-1} - 2\zeta_d)$ and $P(s) = 1$. This controller is a feedback from roll rate and is hence realisable. The bi-quadratic part of controller with complex poles given by the zeros of the specification and complex zeros given by the poles of the roll dynamics of the vessel, was suggested in Blanke et al. (2000), where ability was demonstrated to tune to variations in roll motion spectra met in costal areas in Denmark. The main tuning parameter is ω_d and tuning is easily achieved to different sea conditions, on the condition that there is a separation of around a factor 3 or more between the ω_d and the RHP zero, at q. Figure 4 shows the sensitivity function calculated from an identified dynamic model of a Danish SF300 vessel. The RHP zero at the medium speed condition was identified to be $q = 0.18 rad/s$. To cope with changes in the roll disturbance spectrum, a bank of 4 controllers were implemented, and the navigator would selected according to the roll period where maximal damping was desired.

6.3 Gyrostabilisers

A gyrostabiliser consists of a one or more spinning masses rotating at a constant angular velocity ω_s. These devices are located in on the hull in such a way that a gyroscopic torque produced by a gyrostabiliser on the vessel opposes the roll moment generated by the waves. This gyroscopic torque is generated by conservation of angular momentum. The wave-pressure forces on the hull induce roll motion and an excitation torque on the gyro that is proportional to the roll rate. This excitation torque changes the angular momentum such that the spinning wheels develop precession motion. The cross product of the spin angular velocity and the precession rate induce a torque that opposes the excitation torque, and thus the roll excitation moment on the vessel (Arnold and Maunder, 1961).

The use of twin counter spinning masses prevents gyroscopic coupling with other degrees of freedom. Hence, the

control design for gyrostabilisers can be based on a linear single degree freedom model for roll. The coupled vessel-roll and gyro model can be expressed as:

$$\dot{\phi} = p,$$
(80)
$$K_{\dot{p}} \dot{p} + K_p p + K_\phi \phi = K_w - nK_g \dot{\alpha} \cos\alpha$$
(81)
$$I_p \ddot{\alpha} + B_p \dot{\alpha} + C_p \sin\alpha = K_g p \cos\alpha + T_p$$
(82)

Equation (81) represents the roll dynamics, whereas equation (82) represents the dynamics of the gyrostabiliser about the precession axis, where α is the precession angle, n is the number of spinning masses I_p is inertia, B_p is the damping, and C_p is the restoring term of the gyro about the precession axis due to location of the gyro centre of mass relative to the precession axis—pendulum.

The model (81)-(82) captures the essential dynamics associated with the coupled system. The wave-induced roll moment K_w excites the roll. As the roll motion develops, the roll rate induces a torque along the precession axis of the gyrostabiliser. As the precession develops, there is reaction torque done on the vessel that opposes the wave-induced torque. The later is the roll stabilising torque [1],

$$X_g \triangleq -nK_g \dot{\alpha} \cos\alpha.$$
(83)

Note that this roll moment can only be controlled indirectly through the precession dynamics in (82) via the precession control torque T_p. In the analysis presented in this paper, it is assumed that the spin angular velocity ω_{spin} is constant; and thus the spin angular momentum $K_g = I_{spin}\omega_{spin}$ is constant. The dimensioning of the gyro $(\omega_{spin}, I_{spin})$ is outside the scope of the paper.

The precession control torque T_p is used to control the gyro. As observed by Sperry (Chalmers, 1931), the intrinsic behaviour of the gyrostabiliser is to use roll rate to generate a roll moment. Hence, we could design a precession torque controller such that from the point of view of the vessel, the gyro behaves as damper, that is,

$$T_p : \dot{\alpha}\cos\alpha \approx \beta p, \quad \beta > 1,$$
(84)

Then the coupled equations (81) -(82) simplify to

$$\dot{\phi} = p,$$
(85)
$$K_{\dot{p}} \dot{p} + (K_p + nK_g\beta) p + K_\phi \phi = K_w.$$
(86)

Perez and Steinmann (2009) propose a control design based on gyro-precession information only

$$T_p = -K_{\dot{\alpha}} \dot{\alpha} - K_\alpha \alpha,$$
(87)

which achieves the above goal and ensure stability. With this controller, the precession rate to roll rate transfer function takes the form

$$G_{\alpha\phi}(s) = \frac{\dot{\alpha}(s)}{\dot{\phi}(s)} = \frac{K_g s}{I_g s^2 + (B_g + K_{\dot{\alpha}})s + (C_g + K_\alpha)},$$
(88)

with the necessary and sufficient condition for its stability being $B_g + K_{\dot{\alpha}} > 0$ and $C_g + K_\alpha > 0$. Since this transfer function is positive real, and the ship transfer function from roll moment to roll rate is also positive real, their feedback interconnections is passive and thus stable Perez and Steinmann (2009).

Depending on how the precession torque is delivered, it may be necessary to constraint precession angle and rate. This is outside the scope of this paper.

---

[1] A torque is the moment of a couple—a set of two forces with null resultant.

7. CONCLUSION AND RESEARCH OUTLOOK

In this paper, we have provided a tutorial on control aspects of roll motion control devices. These aspects include the type of mathematical models used to design and analyse the control problem, the inherent fundamental limitations and constraints that some of the designs may be subjected to, and how the performance of the controlled vessels is assessed. In the case of rudder roll damping, a formulation that allows one to assess the potential applicability of this technique was also revisited.

As a research outlook, one of the key issues in roll motion control is the adaptation to the changes in the environmental conditions. As the vessel changes speed and heading, or as the seas build up or abate, the dominant frequency range of the wave-induced forces can change significantly. Due to the fundamental limitations discussed in this paper, a non-adaptive controller may produce roll amplification rather than roll reduction. This topic has received some attention in the literature via multi-mode control switching, but further work in this area could be beneficial. Also on the topic of adaptation, some vessels use trim-flaps and interceptors to set the trim of the vessel, and they provide an opportunity for pitch and also roll control. The change in trim, affects the roll restoring coefficients, and therefore a shift in the vessel natural frequency in roll, which can affect the performance of the roll controller.

In the past few years, new devices have appeared for stabilisation at zero speed, like flapping fins and rotating cylinders. Also the industry's interest in roll gyrostabilisers have been re-ignited. The investigation of control designs for these devices has not yet received much attention within the control community. Hence, it is expected that this will create a potential research activity.

In some sailing conditions, the wave passage along the hull and the wave excited vertical motions result in large variations of the roll restoring strength. These changes in the restoring terms coupled with a exchange of energy between roll and pitch can result in a rapid build up of roll for some vessels reaching angles up to 40 deg in just a few roll cycles. In a mathematical model, this physical effect can be described by a time-change in the roll restoring parameters; and therefore, the phenomenon is often described as roll parametric resonance, or simply parametric roll. In the past 5 years, a significant attention has been put into early detection of this phenomenon, and some control proposals to reduce parametric roll are starting to appear in the literature. It is expected that this interesting non-linear problem will continue to be an area of intense research activity.

REFERENCES

Abkowitz, M. (1964). Lecture notes on ship hydrodynamics–steering and manoeuvrability. Tech. report hy-5, Hydro and Aerodynamics Laboratory Lyngby, Denmark.

Allan, J. (1945). Stabilisation of ships by activated fins. *Transactions of The Royal Institution of Naval Architects RINA*, 87, 123–159.

Arnold, R. and Maunder, L. (1961). *Gyrodynamics and its Engineering Applications*. Academic Press, New York and London.

Baitis, A. (1980). The development and evaluation of a rudder roll stabilization system for the WHEC Hamilton class. Technical Report DDDTNSRDC/SPD-0930-02, DTNSRDC, Bethsada, MD.

Blanke, M. (1981). *Ship propulsion losses related to automatic steering and prime mover control*. Ph.D. thesis, Servolaboratory, Technical University of Denmark.

Blanke, M., Adrian, J., Larsen, K., and Bentsen, J. (2000). Rudder roll damping in coastal region sea conditions. In *Proc. of 5th IFAC Conference on Manoeuvring and Control of Marine Craft, MCMC'2000*.

Blanke, M. and Christensen, A. (1993). Rudder roll damping autopilot robustness to sway-yaw-roll couplings. *In: Proc. of 10th SCSS, Ottawa, Canada*, 93–119.

Blanke, M., Haals, P., and Andreasen, K. (1989). Rudder roll damping experience in Denmark. In *Proc. of IFAC workshop CAMS'89, Lyngby, Denmark*.

Blanke, M. and Knudsen, M. (2006). Efficient parametrization for grey-box model identification - a principal components approach. In *14th IFAC Symposium on System Identification*.

Carley, J. (1975). Feasibility study of steering and stabilising by rudder. *4rd Ship Control System Symposium–SCSS, The Netherlands*.

Chalmers, T. (1931). *The Automatic Stabilisation of Ships*. Chapman and Hall, London.

Conolly, J. (1969). Rolling and its stabilization by fins. *Transactions of The Royal Institution of Naval Architects*, 111.

Cowley, W. (1972). Development of an autopilot to control yaw and roll. *3rd Ship Control System Symposium–SCSS, Bath, UK*.

Cowley, W. and Lambert, T. (1972). The use of a rudder as a roll stabiliser. *3rd Ship Control System Symposium–SCSS, Bath, UK*.

Cowley, W. and Lambert, T. (1975). Sea trials on a roll stabiliser using the ship's rudder. *4th Ship Control System Symposium–SCSS, The Netherlands*.

Dallinga, R. (1993). Hydromechanic aspects of the design of fin stabilisers. *Transactions of The Royal Institution of Naval Architects*.

Fedyaevsky, K. and Sobolev, G. (1964). *Control and Stability in Ship Design*. State Union Shipbuilding, Leningrad.

Fossen, T. (1994). *Guidance and Control of Ocean Marine Vehicles*. John Wiley and Sons Ltd, New York.

Fossen, T. (2002). *Marine Control Systems: Guidance, Navigation and Control of Ships, Rigs and Underwater Vehicles*. Marine Cybernetics, Trondheim.

Frahm, H. (1911). Results of trials of anti-rolling tanks at sea. *Trans. of the Institution of Naval Architects*, 53.

Freudenberg, J.S. and Looze, D.P. (1985). Right half-plane poles and zeros and design trade-offs in feedback systems. *IEEE Transactions on Automatic Control Engineering Practice*, AC-30, 555–565.

Freudenberg, J.S. and Looze, D.P. (1988). *Frequency Domain Properties of Scalar and Multivariable Feedback Systems*. Springer Verlag New York.

Gaillarde, G. (2002). Dynamic behavior and operation limits of stabilizer fins. In *IMAM International Maritime Association of the Mediterranean, Creta, Greece*.

Gawad, A., Ragab, S., Nayfeh, A., and Mook, D. (2001). Roll stabilization by anti-roll passive tanks. *Ocean*

Engineering, 28, 457–469.

Goodrich, G. (1969). Development and design of passive roll stabiliser. *Trans. of The Royal Institution of Naval Architects*, 81–88.

Hearns, G. and Blanke, M. (1998a). Quantitative analysis and design of a rudder roll damping controller. In *Proc. IFAC CAMS'98*.

Hearns, G. and Blanke, M. (1998b). Quantitative analysis and design of a rudder roll damping controller. Technical report, Aalborg University.

Hickey, N. (1999). *Control design for fin roll stabilisation*. Ph.D. thesis, University of Strathclyde, Glasgow, UK.

Hickey, N., Grimble, M., Johnson, M., Katebi, M., and Melville, R. (1997). Robust fin roll stabilisation of surface ships. In *Proc. of the 36th Conference on Decision and Control 1997, San Diego, California, USA*.

Hickey, N., Grimble, M., Johnson, M., Katebi, M., and Wood, D. (1995). $\mathcal{H}_\infty$ fin roll control system design. In *Proc. of IFAC Conference on Control Applications in Marine Systems, Tronheim, Norway*.

Hickey, N., Johnson, M., Katebi, M., and Grimble, M. (1999). PID controller optimisation for fin roll stailisation. In *Proc. of the International Conference on Control Applications, Hawai, USA*.

Ikeda, Y. (2004). Prediction methods of roll damping of ships and their application to determine optimum stabilisation devices. *Marine Technology*, 41(2), 89–93.

Ikeda, Y., Komatsu, K., Himeno, Y., and Tanaka, N. (1976). On roll damping force of ship: Effects of friction of hull and normal force of bilge keels. *J. Kansai Society of Naval Architects*, 142, 54–66.

Källström, C. (1981). Control of yaw and roll by rudder/fin stabilization system. In *Proc. of 6th International Ship Control System Symposium (SCSS'81)*.

Källström, C., Wessel, P., and Sjölander, S. (1988). Roll reduction by rudder control. In *Spring Meeting*-STAR *Symposium, 3rd IMSDC*.

Katebi, M., Hickey, N., and Grimble, M. (2000). Evaluation of fin roll stabilizer design. In *5th IFAC Conference on Manoeuvring and Control of Marine Craft MCMC'00*, 31–37.

Lamb, H. (1932). *Hydrodynamics*. Cambridge University Press, First edition piblished in 1879; Sixth edition published in 1932. First Cambridge University Press paper back edition published in 1993. edition.

Lloyd, A. (1989). *Seakeeping: Ship Behaviour in Rough Weather*. Ellis Horwood.

Lloyd, A. (1975a). Roll stabilisation by rudder. *4th Ship Control System Symposium–SCSS, The Netherlands*.

Lloyd, A. (1975b). Roll stabiliser fins: A design procedure. *Trans. of The Royal Institution of Naval Architects*.

Minorsky, N. (1935). Problems of anti-rolling stabilization of ships by the activated tank method. *American Society of Naval Engineers*, 47.

Monk, K. (1988). A war ship roll criterion. *Royal Institute of Naval Architects*, 219–240.

NATO (2000). *Standarization Agreement: common procedures for seakeeping in the ship design process (*STANAG*) 3rd ed N0.4154*. North Atlantic Treaty Organization (NATO), Military Agency for Standarization.

Norrbin, N. (1970). Theory and observation on the use of a mathematical model for ship manoeuvring in

deep and confined waters. *8th Symposium on Naval Hydrodynamics, USA*.

Ochi, M. (1998). *Ocean Waves: The Stochastic Approach*. Ocean Technology Series. Cambridge University Press.

Perez, T. (2005). *Ship Motion Control*. Advances in Industrial Control. Springer-Verlag, London.

Perez, T. and Goodwin, G. (2008). Constrained predictive control of ship fin stabilizers to prevent dynamic stall. *Control Engineering Practice*, 16, 482–494.

Perez, T. and Revestido-Herrero, E. (2010). Damping structure selection in nonlinear ship manoeuvring models. In *8th IFAC Conf. on Control Applications in Marine Systems, CAMS 2010, Rostock, Germany*.

Perez, T. and Steinmann, P. (2009). Analysis of ship roll gyrostabiliser control. In *8th IFAC International Conference on Manoeuvring and Control of Marine Craft. September, Guaruja, Brazil*.

Price, W. and Bishop, R. (1974). *Probabilistic Theory of Ship Dynamics*. Chapman and Hall, London.

Roberts, G.N. (1993). A method to determine the applicability of rudder roll stabilization for ships. *In Proc. of IFAC World Congress*, 5, 405–408.

Roberts, J. and Spanos, P. (1990). *Random vibration and statistical linearization*. John Wiley and Sons.

Ross, A. (2008). *Nonlinear Maneuvering Model Based on Low-Aspect Ratio Lift Theory and Lagrangian Mechanics*. Phd thesis., Dept. of Engineerign Cybernetics.

Schlick, O. (1904). Gyroscopic effects of flying weels on board ships. *Transactions of The Institution of Naval Architects INA*.

Sellars, F. and Martin, J. (1992). Selection and evaluation of ship roll stabilization systems. *Marine Technology, SNAME*, 29(2), 84–101.

Serón, M., Braslavsky, J., and Goodwin, G. (1997). *Fundamental Limitations in Filtering and Control*. Springer.

Skejic, R. (2008). *Maneuvering and Seakeeping of a Sinlge Ship and of Two Ships in Interaction*. PhD thesis 2008:55, Department of Marine Technology. Norwegian University of Science and Technology (NTNU), Trondheim, Notrway.

St Denis, M. and Pierson, W. (1953). On the motion of ships in confused seas. *SNAME Trans.*, 61, 280–332.

Taggart, R. (1970). Anomalous behavior of merchant ship steering systems. *Marine Technology*, April, 205–215.

van Amerongen, J., van der Klugt, P., and van Nauta Lemke, H. (1990). Rudder roll stabilization for ships. *Automatica*, 26, 679–690.

van der Klught, P. (1987). *Rudder roll stabilization*. Ph.D. thesis, Delft University of Technology, The Netherlands.

van Gunsteren, F. (1974). Analysis of roll stabilizer performance. *Trans. of The Society of Naval Architects and Marine Engineers*, 21, 125–146.

Vasta, J., Giddings, A., Taplin, A., and Stilwell, J. (1961). Roll stabilization by means of passive tanks. *Transactions of The Society of Naval Architects and Marine Engineers SNAME*, 69, 411–439.

Watt, P. (1883). On a method of reducing the rolling of ships at sea. *Trans. of the Institution of Naval Architects*, 24.

Watt, P. (1885). The use of water chambers for reducing the rolling of ships at sea. *Trans. of the Institution of Naval Architects*, 26.